The influence of positronium photoionization rate on the polar cap X-ray luminosity of radio pulsars

A.I.Tsygan[1], D.P.Barsukov[1], M.V.Vorontsov[2]

[1] *Ioffe Institute* [2] *SPbPU*

The influence of positronium photoinization rate on the polar cap X-ray luminosity of old radio pulsars is considered. It is assumed that polar cap is heated only by reverse positrons, accelerated in pulsar diode. It is supposed that pulsar diode is in stationary state with lower plate on star surface (polar cap model), occupies all pulsar tube crosssection and operates in regime of steady space charge limited electron flow. The influence of small scale magnetic field on electric field inside pulsar diode is taken into account. The reverse positron current is calculated in the framework of two models: rapid [1] and gradually screening [2, 3]. To calculate the electron-positron pairs production rate we take into account only the curvature radiation of primary electrons and its absorption in magnetic field. It is assumed that part of electro-positron pairs may be created in bound state (positronium). And later such positroniums are photoionized by thermal photons from polar cap.

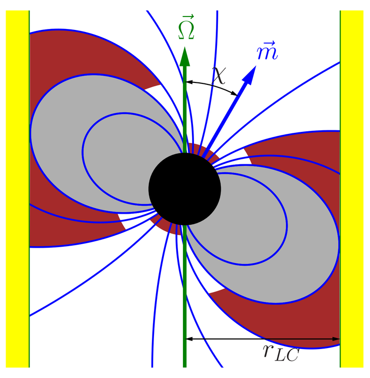

1. **Old isolated radiopulsars**
   $B_{dip} \sim 10^{11} - 10^{12} G$
   $P \sim 100ms - 1s$
   $\tau = P/(2\dot P) \gtrsim 10^6$ years
2. **Goldreich-Julian model**
3. **inner gaps**
4. **free electron emission from neutron star surface**
   small surface magnetic field
   $B_{surf} < 10^{13} G$
   hot polar caps $T \sim (1-3)\cdot 10^6 K$
   Z.Medin, D.Lai (2007)
   $\vec\Omega\cdot\vec m > 0$, $\Omega = \frac{2\pi}{P}$
   $\vec\Omega$ is angular velocity of star
5. **no vacuum gaps, no sparks**
   steady space charge limited flow
   W.M.Fawley, J.Arons, E.T.Scharlemann (1977)
6. **stationary case**
7. **only curvature radiation**
   the inverse compton scattering and synchrotron emission do not taken into account
8. **only photon absorption in magnetic field**
   no photon splitting, photon scattering

Small scale magnetic field

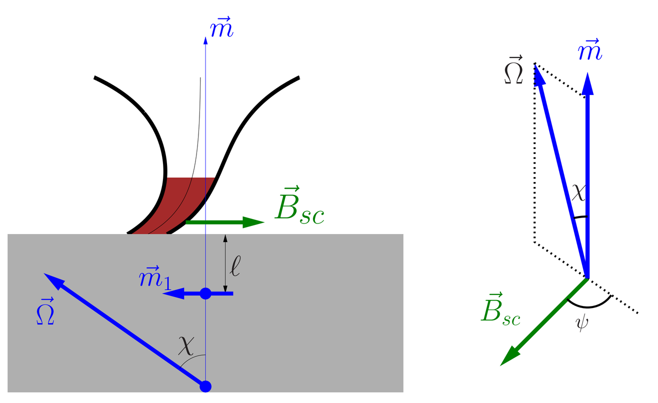

$$\vec B = \frac{3\vec r(\vec r\cdot\vec m) - \vec m r^2}{r^5} + \frac{3\vec\rho(\vec\rho\cdot\vec m_1) - \vec m_1\rho^2}{\rho^5}$$

$$\vec\rho = \vec r - (r_{ns} - \ell)\vec e_z,\quad \vec m = m\vec e_z,\quad \vec m_1 = \nu\left(\frac{\ell}{r_{ns}}\right)^3 m\vec e_x$$

$$\ell = \tfrac{1}{10} r_{ns} \qquad \nu = \frac{B_{sc}}{B_{dip}} \lesssim 1 \qquad 0 \le \psi \le \frac{\pi}{2}$$

Rapid screening model

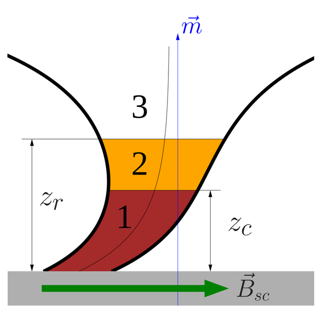

J.Arons, E.T.Scharlemann ApJ **231** 854 (1979)

1. $0 < z < z_c$ acceleration region
   no pairs production, no pair plasma
   large $E_{||} = (\vec E\cdot\vec B)/B$
2. $z_c < z < z_r$ partial screening area
   pair plasma, small $E_{||}$
   positrons return to the polar cap
3. $z > z_r$ full screening area
   pair plasma, $E_{||} = 0$
   no positrons return

Condition

(a) $E_{||}\big|_{z=z_r} = 0$
electric field is continous

(b) $(\vec B\cdot\vec\nabla)E_{||}\big|_{z=z_r} = 0$
charge density is continous

Gradual screening model

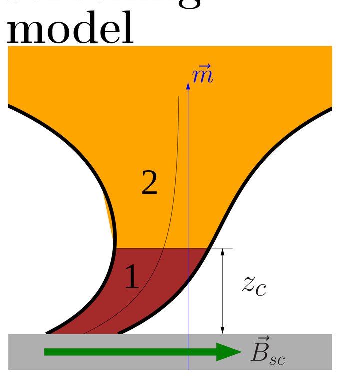

A.K. Harding, A.G. Muslimov ApJ **556** 987 (2001)

The assumptions:

- all values do not depend on time t (stationary case)
- pairs are affected only by average electric field
- $\tilde\rho_{GJ}$ monotonically grows with the altitude z

Hence, conditions $E_{||}\big|_{z=z_r} = 0$ and $(\vec B\cdot\vec\nabla)E_{||}\big|_{z=z_r} = 0$ can not be satisfied at the **same** point

No fullscreening area

There is only partial screening area where the electric field is small and $\Phi \to \Phi_\infty$ at $z \to \infty$

The reverse positron current J2043+2740

rapid: $\tilde\rho_+ \sim 10^{-2}$

$\tilde\rho_+ \lesssim r_t \frac{\partial\tilde\rho_{GJ}}{\partial z}$

gradual: $\tilde\rho_+ \sim 10^{-1}$

$\tilde\rho_+ \approx \frac{1}{2}\left(\tilde\rho_{GJ}(z_f) - \tilde\rho_{GJ}(z_c)\right)$

$z_f - z_c \gtrsim r_{ns} \gg r_t$

$$\rho_+ = \frac{\Omega B}{2\pi c}\tilde\rho_+ \quad\text{and}\quad \rho_{GJ} = -\frac{\Omega B}{2\pi c}\tilde\rho_{GJ}$$

$z_f \sim (1-50) r_{ns}$ is altitude, where plasma waves begin affect on pair dynamics or point of maximum $\tilde\rho_{GJ}$, ρ_+ is charge density of reverse positrons, ρ_{GJ} is Goldreich-Julian density and r_t is radius of pulsar tube, r_{ns} is neutron star radius.

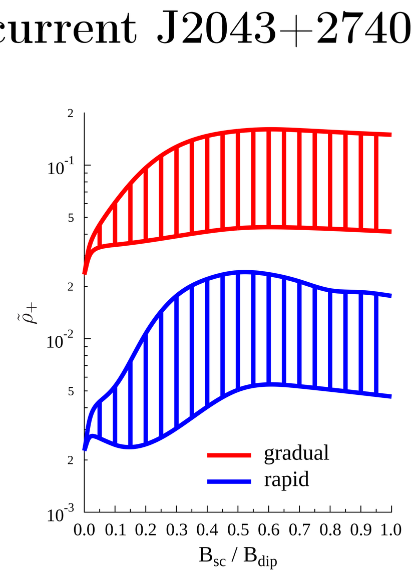

$$B_{dip} = 7.1\cdot 10^{11} G,\ P = 96ms,\ \tau = 1.2\cdot 10^6\ \text{years},\ \chi = 55^\circ$$

The polar cap luminosity J2043+2740

The luminosity L_{pc} of polar cap of J2043+2740 is shown for two values of angle ϕ_Ω and different strenght of small scale magnetic field B_{sc}. ($B_{dip} = 7.1\cdot 10^{11}$ G, $P = 96$ ms, $\tau = 1.2\cdot 10^6$ years, $\dot E = 5.6\cdot 10^{34}$erg/s [5], $\chi = 55^\circ$ [9]) Lower boundaries of dashed areas correspond to $\phi_\Omega = \frac{\pi}{2}$, upper boundaries – to $\phi_\Omega = 0$. Upper limits taken from [10] are shown by green lines, by solid line if we see one cap and by dashed if we see both caps. Luminosity of all star surface taken from [11] is shown by black line.

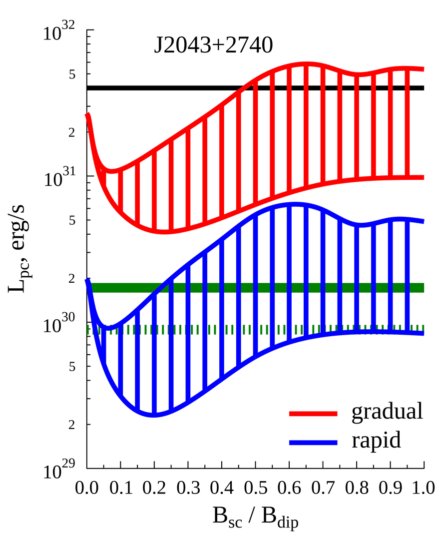

The polar cap luminosity

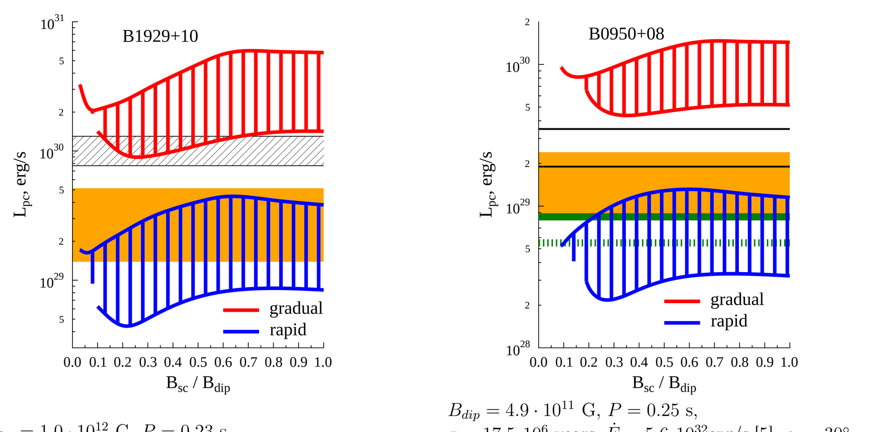

$B_{dip} = 1.0\cdot 10^{12}$ G, $P = 0.23$ s, $\tau = 3\cdot 10^6$ years, $\dot E = 3.9\cdot 10^{33}$erg/s [5], $\chi = 45^\circ$ (β_2, $C < 0$ from [7]) L_{pc} taken from [16] is shown by orange area. L_{pc} taken from [12] is shown by black dashed area.

$B_{dip} = 4.9\cdot 10^{11}$ G, $P = 0.25$ s, $\tau = 17.5\cdot 10^6$ years, $\dot E = 5.6\cdot 10^{32}$erg/s [5] , $\chi = 30^\circ$ [11] L_{pc} taken from [11] are shown by orange area and black lines. Upper limits taken from [10] are shown by green lines, by solid line if we see one cap and by dashed if we see both caps.

The polar cap luminosity

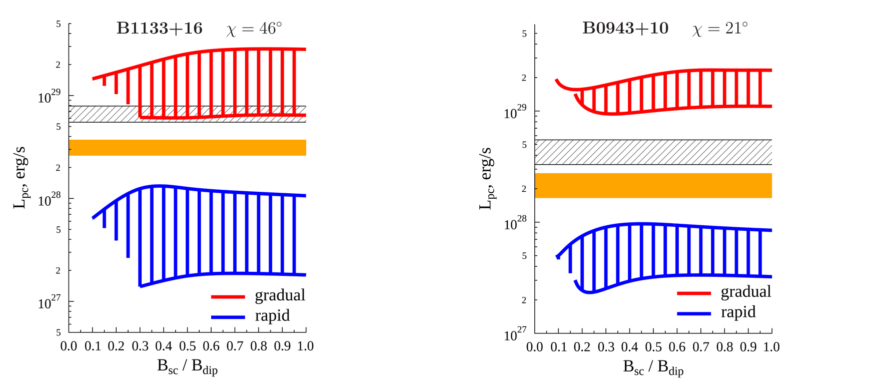

$B_{dip} = 4.26\cdot 10^{12}$ G, $P = 1.188$ s, $\tau = 5.04\cdot 10^6$ years, $\dot E = 8.8\cdot 10^{31}$ers/s [5]. $\chi = 46^\circ$ taken from [8]. X-ray luminosity L_x, taken from [12] is shown by black dashed area, taken from [18] is shown by yellow area.

$B_{dip} = 4.0\cdot 10^{12}$ G, $P = 1.098$ s, $\tau = 4.98\cdot 10^6$ years $\dot E = 10^{32}$erg/s [5]. $\chi = 21^\circ$ taken from [6]. X-ray luminosity L_x, taken from [17] is shown by black dashed area, $0.5\,L_x$ is shown by yellow area.

The polar cap luminosity

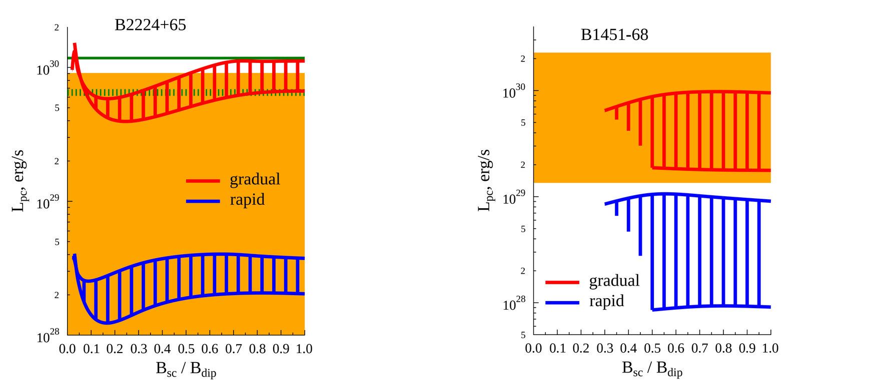

$B_{dip} = 5.2\cdot 10^{12}$ G, $P = 0.68$ s, $\tau = 1.1\cdot 10^6$ years, $\dot E = 1.2\cdot 10^{33}$erg/s [5], $\chi = 16^\circ$ taken from [8] L_{pc} taken from [15] is shown by solid green line. Upper limit taken from [14] is shown by green dashed line and taken from [11] is shown by orange area.

$B_{dip} = 3.2\cdot 10^{11}$ G, $P = 0.26$ s, $\tau = 42.5\cdot 10^6$ years, $\dot E = 2.1\cdot 10^{32}$erg/s [5], $\chi = 50^\circ$ (β_2, $C < 0$ taken from [7]) L_{pc} taken from [19] is shown by orange area.

The polar cap luminosity B0823+26

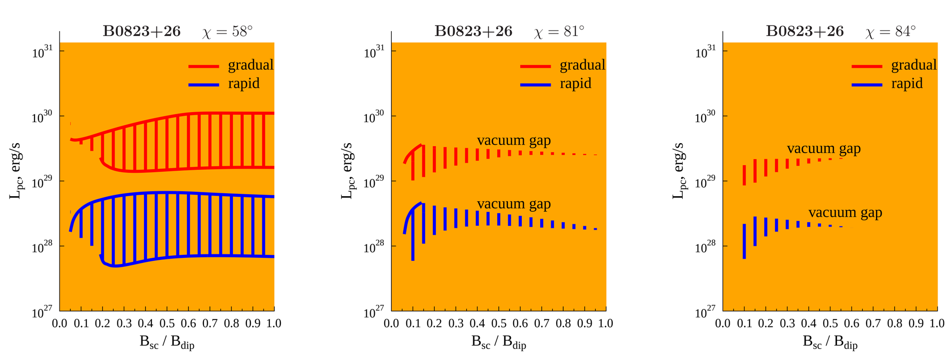

$B_{dip} = 1.9\cdot 10^{12}$ G, $P = 0.53$ s, $\tau = 4.9\cdot 10^6$ years, $\dot E = 4.5\cdot 10^{32}$erg/s [5]. Inclination angle $\chi = 58^\circ$ takes from [6], $\chi = 81^\circ$ takes from [20], $\chi = 84^\circ$ takes from [8]. Upper limit of X-ray luminosity L_x taken from [11] is shown by yellow area.

The polar cap luminosity B0525+21

Fraction P_b of pair created in bounded state we approximate as

1. $P_b = 0$ at $B < B_{low}$
   (no positronium created)
2. $P_b = (B - B_{low})/(B_{high} - B_{low})$
   at $B_{low} \le B \le B_{high}$
3. $P_b = 1$ at $B > B_{high}$
   (all pairs are created in bounded state)

where $B_{low} = 0.04\,B_{cr}$ и $B_{high} = 0.15\,B_{cr}$ [21]
Photoionization rate is assumed to be equal to [21]

$$\frac{dN}{dt} = W_0\left(\frac{10^2}{\Gamma}\right)^3\left(\frac{T}{10^6 K}\right)^2(1 - \cos\theta_{cap})$$

where Γ is positronium lorentz-factor, T is polar cap temperature, θ_{cap} is angular polar cap radius, $W_0 = 6\cdot 10^5 s^{-1}$.

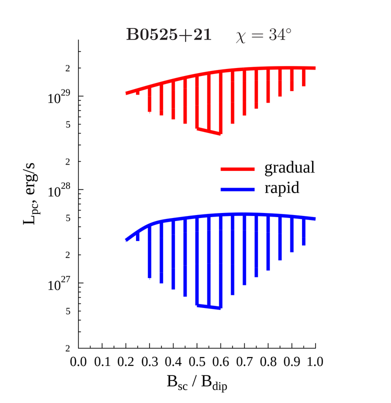

$B_{dip} = 2.5\cdot 10^{13}$ G, $P = 3.74$ s, $\tau = 1.5\cdot 10^6$ years, $\dot E = 3\cdot 10^{31}$erg/s [5], $\chi = 34^\circ$ [6], $W_0 = 6\cdot 10^5 s^{-1}$.

The polar cap luminosity B0525+21

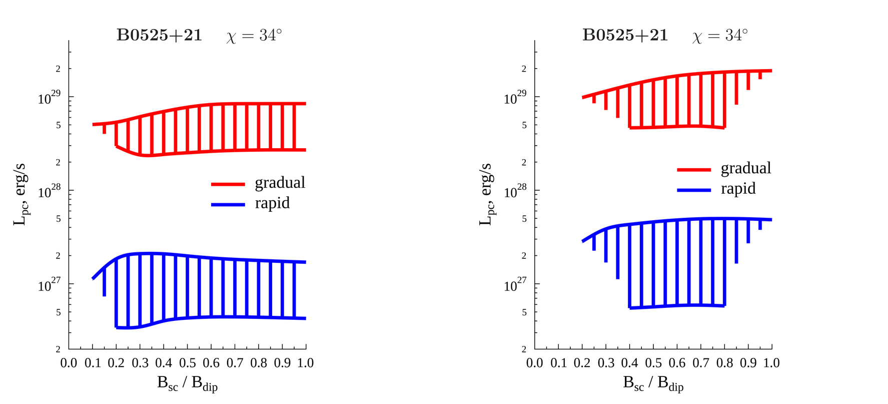

positroniums are not created

$W_0 = 1.2\cdot 10^6 s^{-1}$.

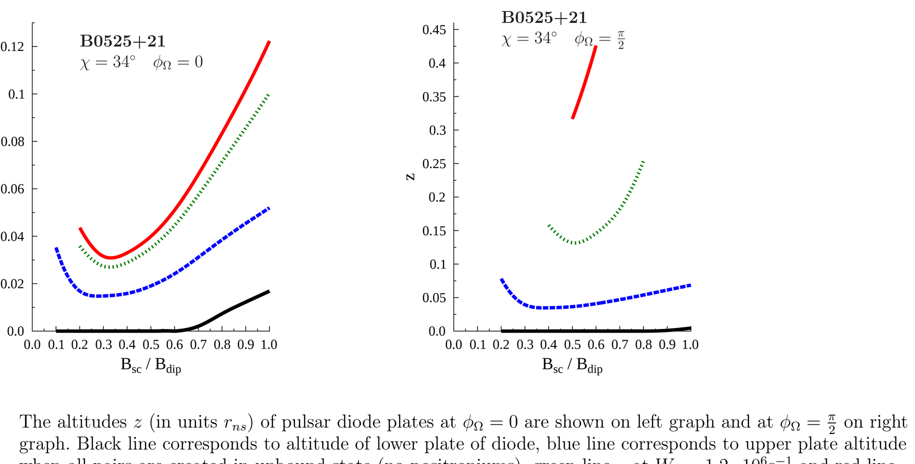

The altitudes z (in units r_{ns}) of pulsar diode plates at $\phi_\Omega = 0$ are shown on left graph and at $\phi_\Omega = \frac{\pi}{2}$ on right graph. Black line corresponds to altitude of lower plate of diode, blue line corresponds to upper plate altitude when all pairs are created in unbound state (no positroniums), green line – at $W_0 = 1.2\cdot 10^6 s^{-1}$ and red line – at $W_0 = 6\cdot 10^5 s^{-1}$.

The polar cap luminosity B0656+14

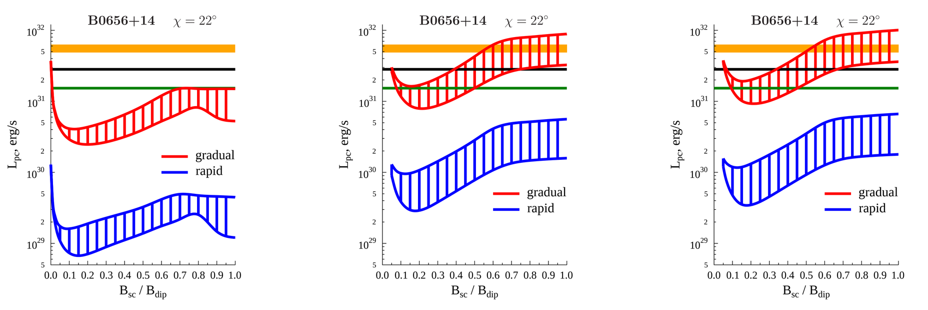

$B_{dip} = 9.3\cdot 10^{12}$ G, $P = 0.385$ s $\tau = 1.1\cdot 10^5$ years, $\chi = 22^\circ$ [7], $\dot E = 3.8\cdot 10^{34}$erg/s [5]. L_{pc} taken from [12] is shown by yellow area, L_{pc} taken from [4] is shown by black line, L_{pc} taken from [13] is shown by green line. The polar cap luminosity in case of all pairs are created in unbound state is shown on left graph, in case of $W_0 = 1.2\cdot 10^6 s^{-1}$ is shown on central graph and in case of $W_0 = 6\cdot 10^5$сек$^{-1}$ is shown on right graph.

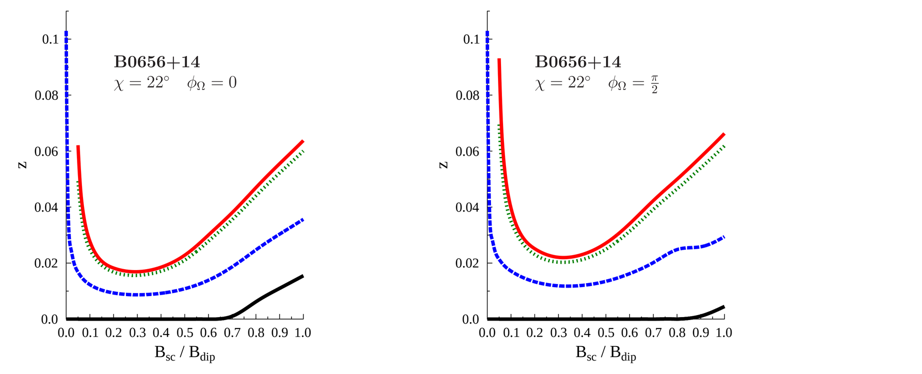

The altitudes z (in units r_{ns}) of pulsar diode plates at $\phi_\Omega = 0$ are shown on left graph and at $\phi_\Omega = \frac{\pi}{2}$ on right graph. Black line corresponds to altitude of lower plate of diode, blue line corresponds to upper plate altitude when all pairs are created in unbound state (no positroniums), green line – at $W_0 = 1.2\cdot 10^6 s^{-1}$ and red line – at $W_0 = 6\cdot 10^5 s^{-1}$.

The polar cap luminosity B0834+06

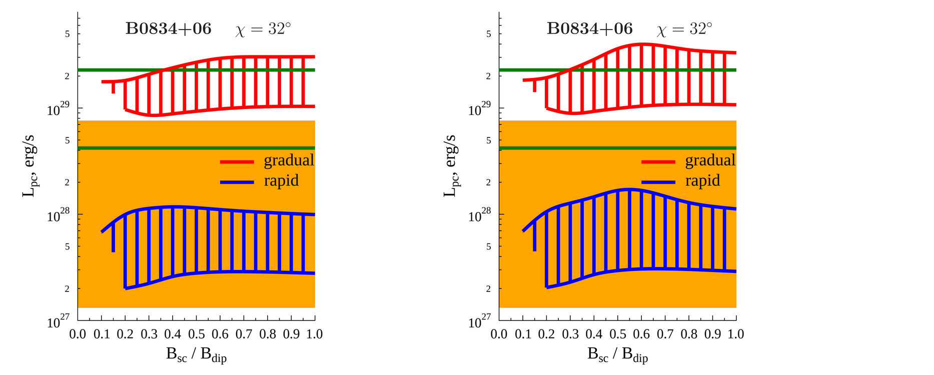

$B_{dip} = 6.0\cdot 10^{12}$ G, $P = 1.27$ s, $\tau = 3.0\cdot 10^6$ years, $\dot E = 1.3\cdot 10^{32}$erg/s [5]. Inclination angle is $\chi = 32^\circ$ (β_1 from [7]). L_{pc} taken from [4] is shown by yellow area, L_{bol} taken from [12] are shown by green lines. The polar cap luminosity in case of all pairs are created in unbound state is shown on left graph and in case of $W_0 = 6\cdot 10^5 s^{-1}$ is shown on right graph. The polar cap luminosity at $W_0 = 1.2\cdot 10^6 s^{-1}$ coinside with the case of $W_0 = 6\cdot 10^5 s^{-1}$.

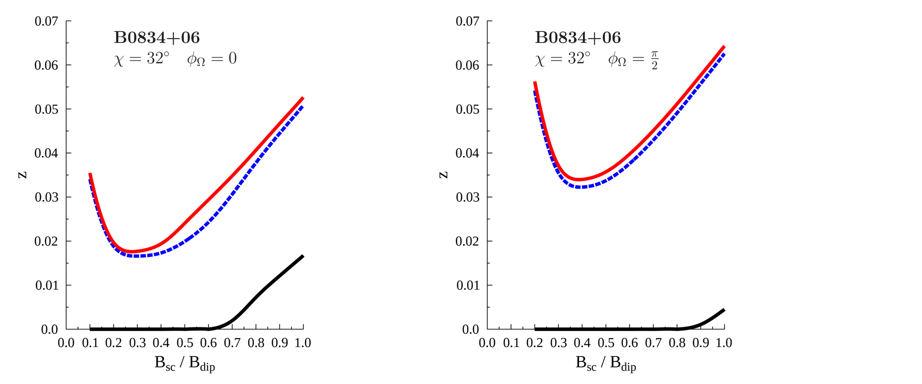

The altitudes z (in units r_{ns}) of pulsar diode plates at $\phi_\Omega = 0$ are shown on left graph and at $\phi_\Omega = \frac{\pi}{2}$ on right graph. Black line corresponds to altitude of lower plate of diode, blue line corresponds to upper plate altitude when all pairs are created in unbound state (no positroniums), upper plate altitude at $W_0 = 6\cdot 10^5 s^{-1}$ is shown by red line. Upper plate altitudes at $W_0 = 1.2\cdot 10^6 s^{-1}$ coinside with the case $W_0 = 6\cdot 10^5 s^{-1}$.

Conclusion

For some pulsars the gradual screening model predicts the polar cap heating which is larger than the observed polar cap luminosity.

Possible explanations:

1. Surface magnetic field $B_{surf} > 10^{14} G$
   no free charge emission
   vacuum gaps, sparks [22]
2. Inner gaps occupy only small part of pulsar tube [23]
3. Large redshift $r_{ns} < 2r_g$
4. Viscous forces at $z \sim r_t$ [24]
   Backflowing radiation [25, 26, 27]
   Radiation locked inside inner gaps [28, 29, 30]
   sound waves from neutron star interior [31]

We sincerely thank O.A. Goglichidze, K.Yu.Kraav, I.F.Malov, V.M.Kontorovich, D.A.Rumyantsev, D.N. Sobyanin, I.F.Malov and V.A.Urpin for help, comments and usefull discussions, I.F. Malov, E.B.Nikitina for provided values of inclination angles, G.G.Pavlov for provided observational data, A.I. Chugunov, M.E.Gusakov, E.M.Kantor, Yu.A. Shibanov, D.A. Zyuzin, A.A. Danilenko, A.Yu.Kirichenko, M.A.Garasyov and D.M.Sedrakian for usefull discussions.

References

[1] Arons J., Fawley W.M., Scharlemann E.T. // ApJ, V.**231** p.854 (1979)
[2] Harding A.K., Muslimov A.G. // ApJ, V.**556** p.987 (2001)
[3] Yu.E. Lyubarskii // A&A V.**261** p.544 (1992)
[4] A. Szary // arXiv:1304.4203
[5] R.N.Manchester et al // Astron. J., V. **129**, p. 1993 (2005) http://www.atnf.csiro.au/research/pulsar/psrcat
[6] I.F. Malov "Radiopulsars"
[7] I.F.Malov, E.B.Nikitina // Astronomy Reports, V. **55**, p.19 (2011)
[8] J.M. Rankin // ApJSS, V. **85**, p. 146 (1993)
[9] A.Noutsos et al // ApJ, V. **728**, p.77 (2011)
[10] W.Becker et al // ApJ, V. **615**, p.908 (2004)
[11] V.E. Zavlin, G.G. Pavlov // ApJ, V. **616**, p. 452 (2004)
[12] J.Gil et al. // ApJ, V. **686**, p. 497 (2008)
[13] G.Pavlov et al // *The Fast and the Furious: Energetic Phenomena in Isolated Neutron Stars, Pulsar Wind Nebulae and Supernova Remnants*, held 22-24 May, 2013 in Madrid, Spain. (2013)
[14] C.Y.Hui, W.Becker // A & A, V. **467**, p.1209 (2007)
[15] C.Y.Hui et al // ApJ, V.**747**, p.74 (2012)
[16] Z.Misanovic et al // ApJ, V.**685**, p.1129 (2008)
[17] B. Zhang, D. Sanwal, G.G. Pavlov // ApJ, V. **624**, p. L109 (2005)
[18] O. Kargaltsev, G.G. Pavlov, G.P. Garmire // ApJ, V. **636**, p. 406 (2006)
[19] B.Posselt et al // ApJ, V.**749**, id 146 (2012)
[20] J.E. Everett, J.M. Weisberg, ApJ, V. **553**, p. 341 (2001)
[21] V.V.Usov, D.B. Melrose // Australian Journal of Physics, V.**48**, p. 571 (1995)
[22] Gil J, Melikidze G I and Geppert U // A&A, V.**407**, p.315 (2003)
[23] S. Shibata // ApJ, V.**378**, p.239. (1991)
[24] S.Shibata et al // MNRAS, V.**295**, L53 (1998)
[25] G.Melikidze, J.Gil // Chin. J. Astron. Astrophys., V.**6**, Suppl. 2, p.81 (2006)
[26] J.Dyks et al // Chin. J. Astron. Astrophys., V.**6**, Suppl. 2, p.85 (2006)
[27] D.Lomiashvili et al // arXiv:0709.2019 (2007)
[28] V.M.Kontorovich, A.B.Flanchik // JETP Letters, V.**85**, p. 267 (2007)
[29] V.M.Kontorovich, A.B.Flanchik // JETP, V. **106**, p.869 (2008)
[30] V.M.Kontorovich, A.B.Flanchik // Astrophysics and Space Science, V. **345**, p. 169 (2013)
[31] D.M.Sedrakyan // "The Modern Physics of Neutron Stars and Relativistic Gravity" Yerevan, Armenia, September 18-21, 2013